JOURNAL OF SOLID STATE CHEMISTRY 69, 258–266 (1987)

The Crystal Structure of $(CH_3)_3NHCdCl_3$ in the High-Temperature (3×3) Phase

SHOJI KASHIDA,[1] YOSHIAKI ITO, AND SHOICHI SATO*

*Department of Physics, Faculty of Science, Niigata University, Niigata 950-21, and *Institute for Solid State Physics, The University of Tokyo, Roppongi Minato-ku, Tokyo 106, Japan*

Received June 22, 1986; in revised form October 20, 1986

The structure of a linear chain compound $(CH_3)_3NHCdCl_3$ is studied at 375 K using three-dimensional X-ray diffraction data. The structure is refined by a block-diagonal least-squares method with the space group $P\bar{6}$. The obtained final R-factor is 0.065 for 2684 reflections. There are nine sublattice sites in the (3×3) unit cell; in eight of these sites, $CdCl_3$ chains are rotated in antiphase, and the last site can be represented by a linear combination of states rotated in the opposite directions (a partially disordered phase). It is also argued that the "ice rule" will be fulfilled in the arrangement of the hydrogen bondings in this structure. © 1987 Academic Press, Inc.

1. Introduction

Recently, it has been found that trimethylamine cadmium trichloride $(CH_3)_3NHCdCl_3$ (abbreviated as TrMCC) undergoes successive structural phase transitions at about 340 and 370 K (*1–4*). The structure is characterized by a hexagonal array of $CdCl_3$ chains and trimethyl (TrM) ions between them (*1*). The transitions are attributed to reorientations of TrM ions, the $CdCl_3$ chains are connected to the TrM ions by the NH · Cl hydrogen bonding, and these chains are rotated mutually in antiphase.

According to the size of the unit cell occupied upon the triangular net, let us denote the lowest-temperature phase as the $(1 \times \sqrt{3})$ phase and the middle phase and the highest-temperature phase as the $(2 \times \sqrt{3})$ and the (3×3) phases, respectively. Figure 1 and Table I show the unit cells and the transition sequence of TrMCC. The (3×2) phase is observed when the sample is cooled from the (3×3) phase.

In this report, we present refinement of the high-temperature (3×3) structure of TrMCC based on three-dimensional data which were collected on a four-circle diffractometer.

2. Experimental

Single crystals of $(CH_3)_3NHCdCl_3$ were prepared at room temperature by a slow cooling of aqueous solution containing stoichiometric amounts of $(CH_3)_3NHCl$ and $CdCl_2$. By cutting and etching with water, the crystal was shaped into a sphere with a diameter of about 0.40 mm and mounted on a Rigaku automatic four-circle diffractometer. The sample was heated in a stream of

[1] To whom correspondence should be addressed.

0022-4596/87 $3.00

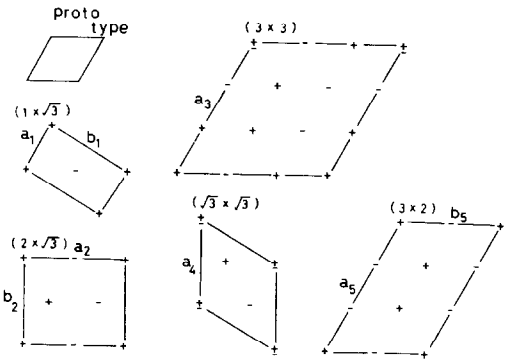

FIG. 1. Schematic representation of the geometrical relationship between the unit cells found in $(CH_3)_3NHCdCl_3$ (TrMCC) and $(CH_3)_3NHCdBr_3$ (TrMCB). Signs represent rotational directions of the metal–halogen chain: + is clockwise, − is counterclockwise, and ± is a linear combination of these two states.

hot air, and the temperature was kept constant at about 375 K. Unit cell parameters were derived by least squares from measurements of 11 reflections within the range $22° < 2\theta < 37°$ (MoK_α). The obtained unit cell dimensions are given in Table I; these values are not very accurate, since the crystal was cracked when passed through the (3 × 3) transition and split peaks were often observed. These values were, however, sufficient for the data collection.

Intensity data were collected using MoK_α radiation monochromated by a graphite crystal. The reflections were scanned in the θ–2θ mode. Since the peaks were split, as mentioned, the scanning range was taken broader than usual as $\Delta 2\theta = 4.0° + 1.2 \tan \theta$; the scanning rate was 4° per minute. Some interference with other Bragg peaks is anticipated because the wavelength used (0.7107 Å) is relatively short in comparison with the lattice constant $a \simeq 26$ Å. In the present case, however, the $h00$ reflections with $h \neq 3n$ are very weak and this overlapping has little effect upon the data. The backgrounds were measured for 10 sec at each limit of the scan range. Three standard reflections, 12 0 0, 0 12 0, and 0 0 4, were monitored every 50 reflections. There was no significant change in the intensity of the standard reflections throughout the data collection.

Intensities of 3512 accessible reflections up to $2\theta = 55°$ with indices $(+h, +k, +l)$ were collected. The data were corrected for the usual Lorentz and polarization effects. Absorption corrections were made assuming a spherical shape of the sample ($\mu R \simeq 0.6$). Reflections for which the intensities were less than three times the standard deviations were regarded as unobserved and were not included in subsequent calculations. The resulting number of observed reflections was 2688.

3. Structure Determination

There are nine sublattice sites for the $CdCl_3$ chains in the unit cell, and let us de-

TABLE I

TRANSITION SEQUENCE OF $(CH_3)_3NHCdCl_3$

342 K	374 K	Cooling	
$Pbnm(1 \times \sqrt{3})$	$Pbnm(2 \times \sqrt{3})$	$P\bar{6}(3 \times 3)$	$P2_1/m(3 \times 2)$
$(Z = 4)$	$(Z = 8)$	$(Z = 18)$	$(Z = 12)$
$b \simeq \sqrt{3}a_0$	$a \simeq 2a_0$, $b \simeq \sqrt{3}a_0$	$a \simeq 3a_0$	$a \simeq 3a_0$, $b \simeq 2a_0$
$a = 8.99$ Å	$a = 17.12$ Å	$a = 26.03$ Å	$a = 25.69$ Å
$b = 14.50$ Å	$b = 15.26$ Å		$b = 16.91$ Å
$c = 6.71$ Å	$c = 6.73$ Å	$c = 6.735$ Å	$c = 6.71$ Å
(at 300 K)	(at 355 K)	(at 375 K)	(at 300 K)

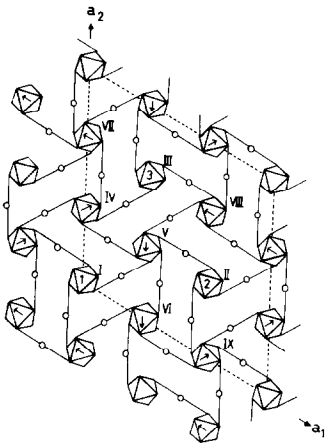

FIG. 2. Previous model for the (3 × 3) phase of TrMCC (*4*); projection along the chain axis. Hexagons and open circles represent Cl_6 octahedra and TrM ions, respectively. Hydrogen bonds are shown by solid lines. Arrows indicate displacements of $CdCl_3$ chains from the symmetrical points such as $\frac{1}{3}$ and $\frac{2}{3}$ along the hexagonal axis *a*.

note these from I to IX as shown in Fig. 2. The usual extinction rule is only $l = 2n + 1$ for $00l$ reflections, and the deduced space group is $P6_3$, $P6_3/m$, or $P6_322$. As reported in the previous study (*4*), neither of these space groups gave plausible structural models which reproduce the observed data. In these space groups, the chains at the sites from IV to IX must be rotated in the same direction.

From a careful survey of the reflection peaks we found that the superlattice reflections are extremely weak in the $(h0l)$ plane and also that the hhl reflections (including the above $00l$ reflections) are hard to observe if $l = 2n + 1$ and $h = 3n$. These pseudoextinction rules means that at least the heavy atoms (Cd and Cl) must fulfill the following conditions: the first extinction means that in the projection along the hexagonal principal axis the $CdCl_3$ chains at sites I to IX are all equivalent, and the second means that in the projection normal to the a–c plane the atoms must be overlapped if their coordinates are shifted $\frac{1}{2}$ along the *c*-axis.

As a model which is consistent with these extinction rules, we have proposed the structure shown in Fig. 2 (*4*): the chains are rotated in antiphase at the sites IV to IX so as to make a two-dimensional antiferrodistortive honeycomb network, and at the sites I to III which are enclosed by this honeycomb network, the rotational mode was assumed to be $++-$. We have taken this model as the start of our refinement and judged that the $00l$ extinction is accidental and it only means that the structure has local 2_1 screws.

In the course of the refinement, however, a partial disorder model was found to agree better with the observed peak intensities; the chain at the site I is represented by a superposition of states rotated in the clockwise and counterclockwise directions. The coordinates of Cd and Cl atoms and their thermal parameters were refined by a block-diagonal least-squares program (*5*) adopting the hexagonal space group $P\bar{6}$. All reflections were given unit weight and the scattering factors of all the atoms were those listed in "International Tables for X-Ray Crystallography" (1974) (*6*). Corrections for anomalous dispersion of Cd and Cl atoms were also included.

The residual index $R = \Sigma(|F_o| - |F_c|)/(\Sigma|F_o|)$ was lowered to 0.13 using anisotropic temperature factors. At this stage, a three-dimensional difference Fourier synthesis using the phases based on the coordinates of Cd and Cl atoms revealed the positions of N and C atoms (Fig. 3). On the plane at $z = 0.5$, we observe gourd-shaped peaks of N atoms (cf. Fig. 3c, IV–VI), which we denote as "type-1 disorder." At $z = 0$, on the other hand, we observe asymmetrically elongated nitrogen peaks (cf. Fig. 3c, I–III): "type-2 disorder." Further, near the origin of the plane at $z = 0$, we observe a single nitrogen peak followed by two carbon peaks (cf. Fig. 3c, II): "type-3

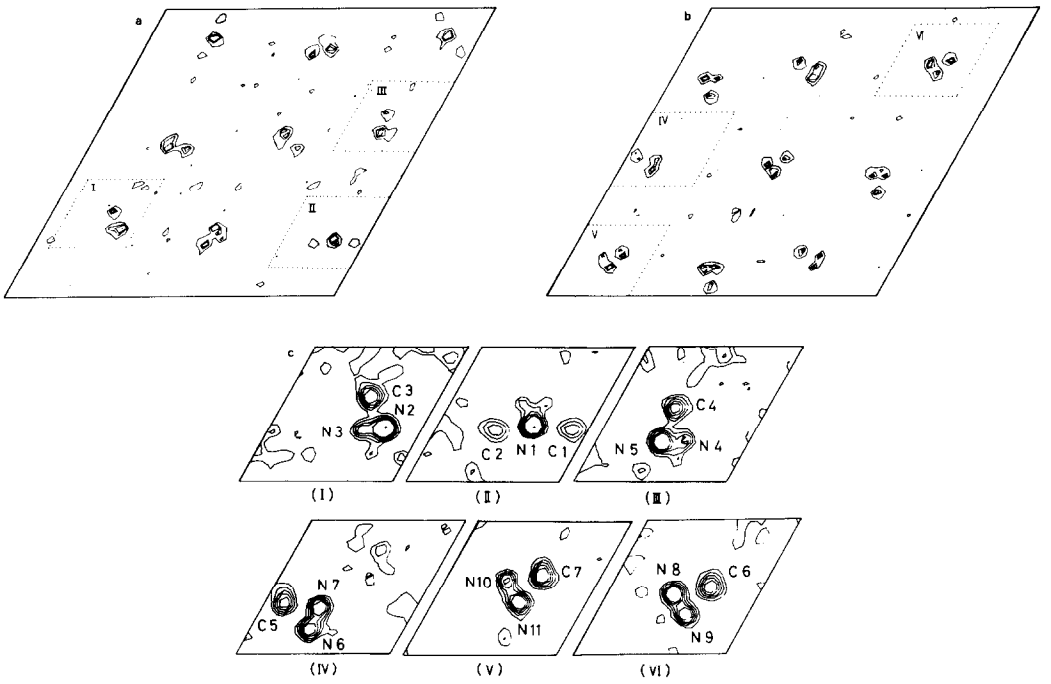

FIG. 3. Section of difference Fourier synthesis of the (3 × 3) structure of TrMCC: (a) $z = 0$, (b) $z = 0.5$, and (c) extended picture of the areas shown by dotted lines. The phases were determined from the coordinates of Cd and Cl atoms.

disorder." A detailed discussion about the nature of these disorders will be given in the next section.

In the subsequent refinement, these light atoms were included; the occupation probability of the atoms was estimated from the peak height appearing in the difference Fourier synthesis. Hydrogen atoms were not detected, probably because of large thermal motions of the methyl groups, therefore, these were not taken into account. In the final stage, four low-angle reflections of relatively high intensity (300, 030, 330, and 004) were suspected to be affected by extinction and were not taken into account in the calculation. The obtained R-factor is 0.066 and $R_w = [\Sigma w(|F_o| - |F_c|)^2/\Sigma w|F_o|^2]^{1/2} = 0.056$ with $w = 1.0$.[2]

For the superlattice reflections ($h \neq 3n$ and $k \neq 3m$) only, the estimated R-factor is 0.127. Final atomic coordinates and thermal parameters are given in Table II, and the bond distances and angles are shown in Table III.

4. Description of the Structure and Discussion

Figure 4 shows the projection of the (3 × 3) structure along the c-axis. Three of the

[2] See NAPS document No. 4458 for 18 pages of supplementary material. Order from ASIS/NAPS. Microfiche Publications, P.O. Box 3513, Grand Central Station, New York, NY 10163. Remit in advance $4.00 for microfiche copy or for photocopy, $7.75 up to 20 pages plus $.30 for each additional page. All orders must be prepaid. Institutions and Organizations may order by purchase order. However, there is a billing and handling charge for this service of $15. Foreign orders add $4.50 for postage and handling, for the first 20 pages, and $1.00 for additional 10 pages of material, $1.50 for postage of any microfiche orders.

TABLE II

ATOMIC COORDINATES AND THERMAL PARAMETERS WITH esd's[a,b]

Atom	X	Y	Z	B_{11}	B_{22}	B_{33}	B_{12}	B_{13}	B_{23}
Cd(1)	0(—)	0(—)	2563(3)	16(0)	16(0)	92(4)	8(0)	0(—)	0(—)
Cd(2)	3333(—)	6667(—)	2558(4)	15(0)	15(0)	88(5)	8(0)	0(—)	0(—)
Cd(3)	6667(—)	3333(—)	2558(4)	16(0)	16(0)	91(4)	8(0)	0(—)	0(—)
Cd(4)	−75(1)	3261(1)	2498(3)	17(0)	17(0)	95(2)	8(0)	1(1)	0(1)
Cd(5)	81(0)	6667(1)	2488(3)	15(0)	17(0)	95(2)	8(0)	−1(1)	0(1)
Cl(1)	204(7)	831(7)	0(—)	31(3)	21(2)	265(47)	15(2)	0(—)	0(—)
Cl(2)	899(4)	312(4)	5000(—)	18(1)	20(1)	220(34)	17(1)	0(—)	0(—)
Cl(3)	608(4)	859(5)	0(—)	8(1)	12(2)	144(27)	3(1)	0(—)	0(—)
Cl(4)	868(5)	509(5)	5000(—)	25(2)	26(2)	207(35)	20(1)	0(—)	0(—)
Cl(5)	3971(2)	6433(2)	0(—)	12(1)	12(1)	118(12)	6(1)	0(—)	0(—)
Cl(6)	2747(3)	6966(3)	5000(—)	21(1)	21(1)	149(14)	15(1)	0(—)	0(—)
Cl(7)	6895(3)	2699(3)	0(—)	22(1)	20(1)	153(15)	15(1)	0(—)	0(—)
Cl(8)	6358(3)	3921(3)	5000(—)	27(1)	26(1)	207(18)	20(1)	0(—)	0(—)
Cl(9)	572(3)	3048(3)	0(—)	14(1)	22(1)	148(14)	8(1)	0(—)	0(—)
Cl(10)	148(3)	4148(3)	0(—)	21(1)	15(1)	148(15)	7(1)	0(—)	0(—)
Cl(11)	−936(3)	2601(3)	0(—)	15(1)	14(1)	171(15)	3(1)	0(—)	0(—)
Cl(12)	−736(3)	3459(3)	5000(—)	17(1)	19(1)	146(15)	9(1)	0(—)	0(—)
Cl(13)	−270(3)	2400(3)	5000(—)	17(1)	10(1)	154(15)	0(1)	0(—)	0(—)
Cl(14)	777(3)	3930(3)	5000(—)	11(1)	15(1)	156(14)	2(1)	0(—)	0(—)
Cl(15)	289(3)	6020(3)	0(—)	22(1)	20(1)	131(14)	15(1)	0(—)	0(—)
Cl(16)	722(3)	7547(3)	0(—)	19(1)	25(1)	124(14)	14(1)	0(—)	0(—)
Cl(17)	−791(3)	6461(3)	0(—)	13(1)	28(1)	177(16)	10(1)	0(—)	0(—)
Cl(18)	−124(3)	7336(3)	5000(—)	14(1)	27(1)	160(16)	11(1)	0(—)	0(—)
Cl(19)	−591(2)	5818(3)	5000(—)	12(1)	16(1)	138(14)	6(1)	0(—)	0(—)
Cl(20)	940(2)	6861(3)	5000(—)	14(1)	24(1)	173(15)	12(1)	0(—)	0(—)
N(1)	1917(12)	981(13)	0(—)	20(5)	22(5)	325(88)	5(4)	0(—)	0(—)
N(2)	2380(14)	4820(17)	0(—)	10(5)	29(8)	70(66)	4(5)	0(—)	0(—)
N(3)	2378(29)	4432(39)	0(—)	12(11)	36(20)	30(113)	4(12)	0(—)	0(—)
N(4)	−1494(17)	4234(16)	0(—)	32(7)	22(5)	254(115)	18(4)	0(—)	0(—)
N(5)	−1091(21)	4220(20)	0(—)	32(7)	27(6)	118(138)	29(4)	0(—)	0(—)
N(6)	995(18)	5572(16)	5000(—)	13(7)	7(6)	212(115)	1(5)	0(—)	0(—)
N(7)	907(18)	5224(18)	5000(—)	25(6)	22(6)	254(144)	19(4)	0(—)	0(—)
N(8)	−2401(17)	1897(16)	5000(—)	17(6)	11(5)	203(114)	9(4)	0(—)	0(—)
N(9)	−2033(18)	2203(20)	5000(—)	7(7)	14(9)	188(111)	−9(7)	0(—)	0(—)
N(10)	1340(18)	2389(18)	5000(—)	24(6)	23(6)	386(185)	20(4)	0(—)	0(—)
N(11)	989(18)	2393(25)	5000(—)	4(6)	28(12)	354(177)	1(7)	0(—)	0(—)
C(1)	1907(31)	1594(31)	0(—)	19(12)	25(14)	449(285)	5(10)	0(—)	0(—)
C(2)	1863(38)	404(28)	0(—)	32(20)	10(11)	387(257)	−4(13)	0(—)	0(—)
C(3)	2947(12)	4830(12)	0(—)	18(4)	18(4)	448(124)	12(3)	0(—)	0(—)
C(4)	−1521(16)	3666(14)	0(—)	26(6)	19(5)	591(180)	11(4)	0(—)	0(—)
C(5)	333(13)	5138(19)	5000(—)	9(4)	34(8)	912(263)	9(4)	0(—)	0(—)
C(6)	−1893(14)	1740(16)	5000(—)	19(5)	29(7)	646(197)	13(4)	0(—)	0(—)
C(7)	1431(20)	3002(13)	5000(—)	45(10)	8(4)	727(224)	10(5)	0(—)	0(—)
C(8)	2035(13)	4468(10)	1952(43)	46(8)	19(4)	265(67)	10(4)	52(17)	11(15)
C(9)	−1135(13)	4627(18)	1701(51)	22(6)	66(11)	371(80)	0(6)	19(19)	−87(23)
C(10)	2243(17)	1260(19)	1985(59)	50(10)	67(13)	337(100)	17(9)	21(30)	−35(34)
C(11)	1260(12)	5534(12)	3240(44)	33(6)	29(6)	230(65)	2(5)	29(17)	−8(18)
C(12)	−2385(13)	2207(11)	3189(38)	53(7)	37(5)	117(45)	22(4)	−23(15)	16(14)
C(13)	950(18)	2037(15)	3386(46)	77(12)	46(8)	198(63)	25(7)	−62(25)	−48(20)

Note: All values are multiplied by 10^4, and the esd's are given in parentheses.

[a] The thermal parameters are of the form $\exp(-B_{11}h^2 - B_{22}k^2 - B_{33}l^2 - 2B_{12}hk - 2B_{13}hl - 2B_{23}kl)$.

[b] The atoms are assumed to have the following weight (others with weight 1): ½: Cl(1), Cl(2), Cl(3), Cl(4), N(6), N(7), N(8), N(9), N(10), N(11), C(1), C(2); ⅔: N(1), N(3); ⅓: N(2), N(4).

TABLE III

Bond distances (Å)

Cd(1)–Cl(1)	2.61(2)	Cd(1)–Cl(2)	2.64(1)
Cd(1)–Cl(3)	2.64(1)	Cd(1)–Cl(4)	2.56(1)
Cd(2)–Cl(5)	2.68(1)	Cd(2)–Cl(6)	2.62(1)
Cd(3)–Cl(7)	2.65(1)	Cd(3)–Cl(8)	2.63(1)
Cd(4)–Cl(9)	2.63(1)	Cd(4)–Cl(10)	2.68(1)
Cd(4)–Cl(11)	2.64(1)	Cd(4)–Cl(12)	2.64(1)
Cd(4)–Cl(13)	2.65(1)	Cd(4)–Cl(14)	2.63(1)
Cd(5)–Cl(15)	2.62(1)	Cd(5)–Cl(16)	2.65(1)
Cd(5)–Cl(17)	2.65(1)	Cd(5)–Cl(18)	2.67(1)
Cd(5)–Cl(19)	2.64(1)	Cd(5)–Cl(20)	2.65(1)
N(1)–C(1)	1.61(9)	N(1)–C(10)	1.56(6)
N(1)–C(2)	1.44(11)		
N(2)–C(3)	1.47(6)	N(2)–C(8)	1.60(6)
N(3)–C(3)	1.32(11)	N(3)–C(8)	1.62(11)
N(4)–C(4)	1.45(6)	N(4)–C(9)	1.51(6)
N(5)–C(4)	1.31(7)	N(5)–C(9)	1.61(7)
N(6)–C(5)	1.52(7)	N(6)–C(11)	1.40(6)
N(7)–C(5)	1.40(7)	N(7)–C(11)	1.47(6)
N(8)–C(6)	1.60(6)	N(8)–C(12)	1.45(6)
N(9)–C(6)	1.43(7)	N(9)–C(12)	1.53(6)
N(10)–C(7)	1.49(7)	N(10)–C(13)	1.46(7)
N(11)–C(7)	1.42(8)	N(11)–C(13)	1.40(8)

Hydrogen bond distances (Å)

Cl(3)(H)–N(1)	3.26(4)	Cl(10)(H)–N(5)	3.33(6)
Cl(12)(H)–N(9)	3.33(5)	Cl(13)(H)–N(11)	3.29(7)
Cl(14)(H)–N(7)	3.22(5)	Cl(20)(H)–N(6)	3.43(5)

Bond angles (deg)

Cl(2)–Cd(1)–Cl(3)	94.69(38)	Cl(3)–Cd(1)–Cl(4)	88.85(42)
Cl(5)–Cd(2)–Cl(6)	176.36(23)	Cl(7)–Cd(3)–Cl(8)	175.70(25)
Cl(5)–Cd(2)–Cl(5′)	82.75(19)	Cl(6)–Cd(2)–Cl(6′)	84.66(23)
Cl(5)–Cd(2)–Cl(6′)	98.64(21)	Cl(7)–Cd(3)–Cl(7′)	82.36(23)
Cl(8)–Cd(3)–Cl(8′)	85.05(25)	Cl(7)–Cd(3)–Cl(8′)	93.73(24)
Cl(9)–Cd(4)–Cl(10)	83.97(25)	Cl(9)–Cd(4)–Cl(12)	179.12(25)
Cl(9)–Cd(4)–Cl(13)	95.67(25)	Cl(10)–Cd(4)–Cl(11)	84.79(24)
Cl(15)–Cd(5)–Cl(16)	84.78(23)	Cl(15)–Cd(5)–Cl(18)	179.43(24)
Cl(15)–Cd(5)–Cl(19)	97.74(22)	Cl(16)–Cd(5)–Cl(17)	83.38(26)
C(1)–N(1)–C(10)	79.19(395)	C(2)–N(1)–C(10)	103.51(482)
C(3)–N(2)–C(8)	106.38(319)	C(4)–N(4)–C(9)	112.99(364)
C(3)–N(3)–C(8)	113.06(690)	C(4)–N(5)–C(9)	115.01(444)
C(5)–N(6)–C(11)	111.35(384)	C(6)–N(8)–C(12)	110.67(340)
C(5)–N(7)–C(11)	114.41(399)	C(6)–N(9)–C(12)	114.49(406)
C(7)–N(10)–C(13)	111.18(409)	C(7)–N(11)–C(13)	119.35(543)

Hydrogen bond angles (deg)

Cl(3)(H)–N(1)–C(2)	110.28(430)	Cl(3)(H)–N(1)–C(10)	110.20(242)
Cl(10)(H)–N(5)–C(4)	104.95(335)	Cl(10)(H)–N(5)–C(9)	115.48(302)
Cl(20)(H)–N(6)–C(5)	98.11(277)	Cl(20)(H)–N(6)–C(11)	109.41(269)
Cl(14)(H)–N(7)–C(5)	106.83(309)	Cl(14)(H)–N(7)–C(11)	106.60(259)
Cl(12)(H)–N(9)–C(6)	105.58(305)	Cl(12)(H)–N(9)–C(12)	108.13(274)
Cl(13)(H)–N(11)–C(7)	104.29(379)	Cl(13)(H)–N(11)–C(13)	105.18(373)

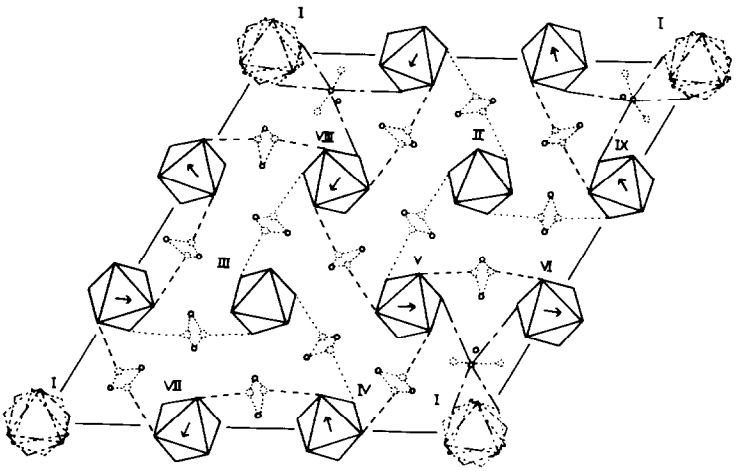

FIG. 4. Schematic drawing of the (3 × 3) structure projected along the chain axis. The dotted hexagons represent Cl_6 octahedra with the weight of $\frac{1}{2}$. Note that at $z = 0$, TrM ions near the origin are linked to the neighboring four Cl atoms (dot-dashed lines), whereas the TrM ions at $z = 0.5$ are linked to only two (dotted lines).

nine $CdCl_3$ chains lie in the threefold axes. This structure model resembles the previous one (Fig. 2); the only difference is that in the present model the $CdCl_3$ chain at the site I is assumed to be disordered.

TrM ions are also disordered as mentioned in the previous section; these ions are turning the directions of the hydrogen bondings between the neighboring Cl atoms. The occupation probability of each hydrogen bonding is 1 : 1 for "type-1 disorder" and 2 : 1 for "type-2 disorder." This type of disorder of TrM ions was first proposed by Chapuis and Zuniga concerning the structure of the $(1 \times \sqrt{3})$ phase (*1*). Because of the orientational disorder of the $CdCl_3$ chains, the TrM ions around site I are linked to four Cl atoms, as shown by the dot-dashed lines in Fig. 4. We observe only a single nitrogen peak and cannot estimate the occupation probability of the hydrogen bond for this "type-3 disorder."

It should be mentioned that the local charge neutrality condition will be fulfilled if we assume an asymmetric occupation of H-bondings for this "type-3 disorder," that is, it consists of two bonds with the weight $\frac{1}{3}$ and the other two with the weight $\frac{1}{6}$; the net charge of the Cd_2Cl_6 molecule is -2, whereas $3 \times \frac{2}{3}$ hydrogens are divided to the sites II to III, $6 \times \frac{1}{3}$ hydrogens to the site I, and $3 \times \frac{1}{2} + \frac{1}{3} + \frac{1}{6}$ hydrogens are divided to the sites IV to IX. The two carbon peaks which are seen in Fig. 3 show indirect but clear evidence that the $CdCl_3$ chains at site I are statistically disordered. Slight displacements of the $CdCl_3$ chains in sites IV to IX, which are represented by arrows in Fig. 4, are interpreted to be due to the hydrogen bondings. The magnitude of these displacements is in fair agreement with those reported previously (*4*).

In recent studies of the successive structural phase transitions of TrMCC and its bromine analogue TrMCB, we have found five phases (*7*); these are the $(1 \times \sqrt{3})$, $(2 \times \sqrt{3})$, (3×3), $(\sqrt{3} \times \sqrt{3})$, and (3×2) phases containing 2, 4, 9, 3, and 6 sites, respectively (cf. Fig. 1). If we define a fictitious spin parameter to represent whether the rotation of the metal–halogen chains is clockwise or counterclockwise, these five

phases can be characterized by Ising-type antiferromagnetic arrangements of spins. In all of these arrangements, the total spin moment disappears; in the case of the structure which contains an odd number of sites such as the (3×3) phase or the $(\sqrt{3} \times \sqrt{3})$ phase, the "partially disordered phase" is realized, where one of the sites can be represented by a linear combination of a +spin state and a −spin state (*7*). The structure has a close resemblance to that observed in linear-chain antiferromagnets such as $CsCoCl_3$ and $CsCoBr_3$, which have a structure similar to that of TrMCC (*8*).

It will be of interest to discuss the similarities and differences in the two cases: arrangement of the rotation of metal–halogen chains and magnetic spins. Let us consider the interaction between the nearest-neighbor $CdCl_3$ chains. There are two TrM ions between them (cf. Fig. 5). Because of the steric constraint, when these chains are rotated in antiphase one of the TrM ions can reorientate and will gain in free energy. This means that the nearest-neighbor interaction is of antiferro type. In the triangular lattice, it is not possible to arrange the chains rotated mutually all in antiphase (the "frustration effect"). Let us divide the hexagonal lattice into a unit triangle which contains three interactions, then the best we can do is to arrange the chains so as not to make triangles with all parallel rotation of chains. This condition is fulfilled in the above five phases observed in TrMCC and TrMCB.

Different from the antiferromagnetic case, however, a ferrimagnetic arrangement (with, for example, two + rotating chains and one − chain) will not be realized. In the present case, because of the charge neutrality condition, it is not possible for more than two TrM ions to be linked to unit chain. In the ferrimagnetic arrangement, all the TrM ions would be bridging between the minority chains and the surrounding majority chains. In order to fulfill the charge neutrality condition, most of the TrM ions must be linked and localized to the majority chains, and will gain little in free energy. In the present circumstance, therefore, it is necessary to seek a stable arrangement which contains equal numbers of + and − spins. The successive phase transitions of TrMCC will be ascribed to an entropy effect. However, in order to clarify the nature of transitions, further microscopic investigations in theory and experiment are necessary.

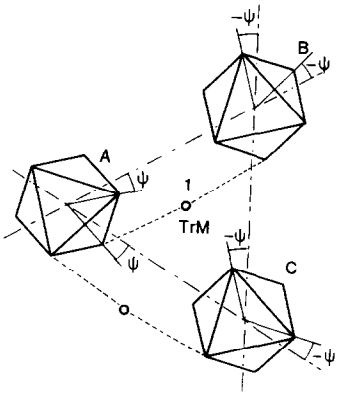

FIG. 5. Schematic representation of the "frustration effect" in the arrangement of rotations of $CdCl_3$ chains in the triangular lattice. If the hexagons A and B are rotated in clockwise and counterclockwise, respectively, from the direction connecting them, the TrM ion at site 1 can reorientate and gain in energy. However, it is not possible to arrange the hexagons A, B, and C rotated mutually all in antiphase, since A and B are in antiphase; if C is rotated in antiphase with A then it must be rotated in phase with B.

Acknowledgment

Part of this work was performed using facilities of the Institute for Solid State Physics of the University of Tokyo.

References

1. G. CHAPUIS AND F. J. ZUNIGA, *Acta Crystallogr., Sect. B* **36,** 807 (1980).
2. U. WALTHER, D. BRINKMANN, G. CHAPUIS, AND H. AREND, *Solid State Commun.* **27,** 901 (1978).

3. S. KASHIDA, K. SANO, T. FUKUMOTO, H. KAGA, AND M. MORI, *J. Phys. Soc. Japan* **52,** 1255 (1983).
4. S. KASHIDA, K. SANO, T. FUKUMOTO, H. KAGA, AND M. MORI, *J. Phys. Soc. Japan* **54,** 211 (1985).
5. T. SAKURAI (Ed.), "UNICS," Japanese Crystallographic Society, Tokyo (1967).
6. "International Tables for X-Ray Crystallography," Vol. IV, Kinoch Press, Birmingham, England (1974).
7. S. KASHIDA AND S. SATO, *J. Phys. Soc. Japan* **55,** 1163 (1986).
8. M. MEKATA, *J. Phys. Soc. Japan* **42,** 76 (1977).